
# Effect of Lubricated Liquid Carbon Dioxide (LCO<inf>2</inf> + MQL) on Grinding of AISI 4140 Steel

Journal of
*Manufacturing and Materials Processing*

MDPI

*Article*

# Effect of Lubricated Liquid Carbon Dioxide ($LCO_2$ + MQL) on Grinding of AISI 4140 Steel

**Deepa Kareepadath Santhosh [1,*], Philipp Hoier [2], Franci Pušavec [1] and Peter Krajnik [1,2]**

[1] Faculty of Mechanical Engineering, University of Ljubljana, 1000 Ljubljana, Slovenia; franci.pusavec@fs.uni-lj.si (F.P.); peter.krajnik@chalmers.se (P.K.)
[2] Department of Industrial and Materials Science, Chalmers University of Technology, 412 96 Gothenburg, Sweden; hoierp@chalmers.se
* Correspondence: deepa.kareepadathsanthos@fs.uni-lj.si

**Abstract:** This paper investigates the potential of utilizing lubricated liquid carbon dioxide ($LCO_2$ + MQL) as an alternative to conventional flood cooling in grinding operations. This approach could facilitate a transition towards fossil-free production, which is a significant challenge in industry. The alternative cooling–lubrication method relies on pre-mixed $LCO_2$ and oil and a single-channel minimum quantity lubrication (MQL) delivery method, which has already demonstrated potential in machining with geometrically defined cutting edges. However, this method has been less explored in grinding. This study primarily evaluates the grindability of AISI 4140 steel, examining surface roughness, residual stresses, microhardness, grinding forces, and specific energy for different cooling–lubrication methods. The results indicate that $LCO_2$ + MQL is capable of attaining surface roughness and microhardness that is comparable to that of conventional flood cooling, especially in the case of less aggressive, finish grinding. Nevertheless, the presence of higher tensile residual stresses in rough grinding suggests that the cooling capability may be insufficient. While the primary objective was to evaluate the technological viability of $LCO_2$ + MQL in terms of grindability, a supplementary cost-effectiveness analysis (CEA) was also conducted to assess the economic feasibility of $LCO_2$ + MQL in comparison to conventional flood cooling. The CEA showed that the costs of both the cooling–lubrication methods are very similar. In conclusion, this study offers insights into the technological and economic viability of $LCO_2$ + MQL as a sustainable cooling–lubrication method for industrial grinding processes.

**Keywords:** grinding; carbon dioxide; cryogenic; cooling; MQL; lubrication



**Citation:** Kareepadath Santhosh, D.; Hoier, P.; Pušavec, F.; Krajnik, P. Effect of Lubricated Liquid Carbon Dioxide ($LCO_2$ + MQL) on Grinding of AISI 4140 Steel. *J. Manuf. Mater. Process.* **2024**, *8*, 230. https://doi.org/10.3390/jmmp8050230

Academic Editor: Steven Y. Liang

Received: 13 August 2024
Revised: 30 September 2024
Accepted: 11 October 2024
Published: 13 October 2024



## 1. Introduction

Grinding is one of the most used operations for finishing precision components. The surface finish of a workpiece is influenced by various factors, including the type of grinding wheel, the abrasive grit size, grinding parameters, and dressing, as well as cooling and lubrication [1]. In order to prevent excessive surface temperatures that can damage the workpiece, the use of metalworking fluids (MWFs) is a common practice during grinding [2]. The MWFs used for grinding are often referred to as grinding fluids. It is well known that grinding fluids assist in cooling and reducing friction between the grinding wheel and the workpiece, which results in reduced temperatures and less wheel wear [3]. The use of MWFs has been criticized due to their negative impact on the environment and operational health and safety risks. Additionally, rising manufacturing costs and regulations are forcing the industry to seek alternatives to conventional cooling–lubrication methods. These alternatives include dry machining, cryogenic cooling, environmentally friendly MWFs, and minimum quantity lubrication (MQL) [4]. These methods fulfill the requirements set forth by the three pillars of sustainability (as shown in Figure 1), namely, social, economic, and environmental [5]. These methods aim to reduce the reliance on harmful MWFs, which will consequently result in a reduction in energy and resource consumption, as well as the carbon emissions that are associated with the use and disposal of MWFs [6].


**Figure 1.** Three pillars of sustainability.

Dry grinding does not provide any cooling or lubrication, and MQL has low cooling capability. As a result, the surface integrity of the component deteriorates, and the workpiece is subject to thermal damage [7]. While cryogenic cooling offers superior cooling, its lubrication capability is insufficient [8]. In view of these limitations, cooling–lubrication methods that combine $LCO_2$ and MQL have been proposed and developed by Hanenkamp et al. [9], where $LCO_2$ provides cooling while MQL provides lubrication. In a study by García et al. [10], the efficiency of grinding AISI 4140 steel using the $CO_2$ + MQL method was compared with dry grinding. Although the results demonstrated that $CO_2$ + MQL led to a notable reduction in wear, the relevance of this comparison is limited by the fact that dry grinding is typically not feasible in real-life production due to excessive heat generation. Mahata et al. [11] studied MQL using soap water in combination with $LCO_2$ for grinding titanium alloys. The study showed that the proposed method resulted in a reduction in grinding forces, improved surface finish, and no visible surface damage when compared to dry grinding and grinding with $LCO_2$. Arafat et al. [12] investigated the application of MQL with supercritical carbon dioxide ($scCO_2$) in the grinding of 100Cr6 bearing steel. The MQL + $scCO_2$ method exhibited similar forces to those of conventional flood cooling, accompanied by higher roughness and more wheel clogging. Liu et al. [13] proposed a method that combines cryogenic air with a biolubricant. The grindability of a titanium alloy was evaluated and compared with dry grinding. Their results showed that for the same grinding parameters, normal forces, tangential forces, specific grinding energy, coefficient of friction, and surface roughness were reduced significantly when using cryogenic air with MQL compared to dry grinding. Balan et al. investigated the effects of dry, MQL, and $LN_2$ + MQL in the grinding of Inconel 751. The use of $LN_2$ + MQL was found to result in a reduction in forces, surface roughness, temperature, and specific energy by 50–65% compared to dry and MQL grinding [14]. A recent study by Sharma et al. employed the use of $LN_2$ + MQL for grinding of AISI D2 tool steel. Here, the $LN_2$ + MQL method was observed to reduce grinding forces, temperature, surface roughness, and specific grinding energy in comparison to conventional and MQL grinding [15].

It was observed that most studies on grinding with combined $LCO_2$ + MQL systems use two separate nozzles for fluid supply. However, the use of such two-channel delivery systems may pose a challenge due to the interactions between $CO_2$ and MQL, which can result in inadequate cooling and lubrication. This is due to the expansion of $CO_2$, pressure, and velocity differences in the media [16]. A recently developed single-channel method that uses pre-mixed $LCO_2$ and oil is less complex than existing systems, easy to implement, and requires moderate $CO_2$ consumption [17]. Although this kind of system has been recently employed in the pin-grinding of cemented carbide materials [18], it has not been explored in conventional grinding applications with a large grinding wheel. This paper addresses this gap by evaluating the impact of the $LCO_2$ + MQL on the grindability of AISI 4140 steel, focusing on surface roughness, residual stresses, microhardness, grinding forces, and specific energy. The objective is to investigate the potential for the industrial application of this novel cooling–lubrication method in grinding. In addition to evaluating the technological viability of $LCO_2$ + MQL, a cost-effectiveness analysis was conducted to provide an initial assessment of the financial feasibility of this technology in comparison

to conventional flood cooling. The insights gained from both the technological and cost analyses provide valuable guidelines for the industrial adoption of $LCO_2$ + MQL.

## 2. Materials and Methods

The workpiece material was AISI 4140 (42CrMo4) steel, which was quenched and tempered to achieve a Vickers hardness of 299 HV1. The workpieces used in the experiments were 10 mm wide and 50 mm long. The chemical composition of the steel is given in Table 1 [19]. AISI 4140 steel was selected for its extensive industrial applications, including in crankshafts, camshafts, and gears [20]. This material is known for its excellent abrasion resistance, high toughness, and high torsional and fatigue strength [21].

**Table 1.** Chemical composition of AISI 4140 (42CrMo4) steel.

| Chemical Composition (Weight %) | | | | | | | |
|---|---|---|---|---|---|---|---|
| **C** | **Si** | **Mn** | **P** | **S** | **Cr** | **Mo** | **Ni** |
| 0.448 | 0.264 | 0.735 | 0.012 | 0.002 | 1.09 | 0.244 | 0.2 |

The grinding experiments were conducted on a Blohm Planomat HP 408 surface grinding machine. The "Norton Quantum Prime" grinding wheel (5NQNX60H 16VS3X) with a diameter of $d_s$ = 400 mm and width 30 mm was used. The grinding wheel was dressed before each experiment using a single-point diamond stationary dresser with a dressing depth of $a_d$ = 0.025 mm and a dressing overlap ratio of $U_d$ = 5.5.

A water-based, solution synthetic fluid (Quakercool 2920 EVC) in 8% concentration was used for conventional flood cooling, which served as a baseline for comparison. Figure 2a shows the experimental setup for flood cooling. The flood cooling was delivered at a pressure of 0.34 MPa (3.4 bar) and a flow rate of 32 L/min. Based on the nozzle geometry, it was estimated that these parameters yielded a fluid velocity of 26 m/s—i.e., 87% of the wheel speed, which is efficient. The two principal methods of conventional grinding fluid delivery are low-pressure (flood) and high-pressure (jet) cooling. The majority of conventional grinders are equipped with low-pressure systems that are relatively simple in design. In contrast, the grinding machine used in this study enables the utilization of higher pressures. Although the employed configuration does not fall into the low-pressure category, it also does not meet the criteria for a high-pressure cooling. Accordingly, the conventional cooling–lubrication method used is designated as "flood cooling". On the other hand, $LCO_2$ + MQL was supplied using the ArcLubeOne system, a novel cooling–lubrication method using a single-channel supply of pre-mixed $LCO_2$ and oil [22]. The lubricant chosen for MQL was HAROLBIO 0, a (petroleum-free) straight synthetic oil with a viscosity index of 152 (ASTM D 2270). The $LCO_2$ was delivered at a mass flow rate of 170 g/min and the oil was delivered at a MQL flow rate of 35 mL/h. In order to prevent phase change in the liquid carbon dioxide in the pipelines, the $LCO_2$ flow rate was set above 80 g/min. A specially designed nozzle has been used for the delivery of $LCO_2$ + MQL into the grinding zone, as shown in Figure 2b.

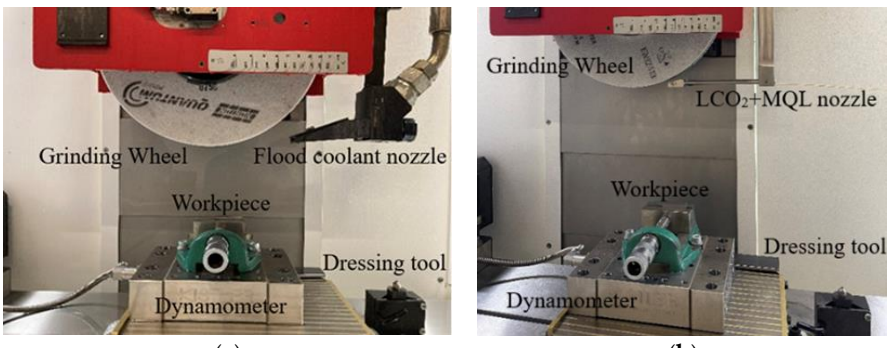


(**a**) (**b**)

**Figure 2.** Experimental setup. (**a**) Flood-cooling method; (**b**) $LCO_2$ + MQL method.

Six grinding experiments were conducted, varying the workpiece speeds from $V_w$ = 10 mm/s to $V$ = 667 mm/s, resulting in varying aggressiveness numbers from a low of $Aggr$ = 1.7 to a high of $Aggr$ = 112. The depth of cut and the wheel speed were kept constant at $a_e$ = 0.01 mm $V_s$ = 30 m/s, respectively. The Aggressiveness number ($Aggr$) was calculated as per Equation (1) [23].

$$Aggr = 10^6 \left(\frac{V_w}{V_s}\right)\left(\frac{a_e}{d_s}\right) \quad (1)$$

where $V_w$ is the workpiece feedrate, $V_s$ is the wheel velocity, $a_e$ is the depth of cut, and $d_s$ is the diameter of the wheel.

The employed grinding parameters and their corresponding aggressiveness numbers are detailed in Table 2.

**Table 2.** Grinding parameters used.

| Experiment No. | Feed Rate (mm/s) | Wheel Speed (m/s) | Depth of Cut (mm) | *Aggr* - | Q′w ($mm^3$/mm/s) |
|---|---|---|---|---|---|
| 1 | 10 | 30 | 0.01 | 1.7 | 0.1 |
| 2 | 50 | 30 | 0.01 | 8.4 | 0.5 |
| 3 | 100 | 30 | 0.01 | 16.8 | 1 |
| 4 | 300 | 30 | 0.01 | 50.4 | 3 |
| 5 | 500 | 30 | 0.01 | 84 | 5 |
| 6 | 667 | 30 | 0.01 | 112 | 6.7 |

The dynamometer (Kistler 9139AA) mounted on the machine table was used to measure the tangential grinding forces ($F_t$) and normal grinding forces ($F_n$).

The portable Mitutoyo surface roughness tester Surftest SJ-210 was used to measure the arithmetic mean height roughness ($R_a$) after each experiment for the different grinding conditions. The measurements were conducted in accordance with the ISO 4287:1997 standard [24], employing a long wavelength cut-off length ($\lambda_c$) of 0.8 mm and a short wavelength cut-off length ($\lambda_s$) of 2.5 µm for the Gaussian filter used. However, ISO 21920-2:2022 [25] has replaced ISO 4287:1997 [24], introducing the concept of the nesting index, where the cut-off wavelength is now considered an example of a nesting index. Three measurements were taken at different points on the workpiece and the average was calculated.

Residual stress measurements were conducted on samples with the lowest and highest $Aggr$ using flood and $LCO_2$ + MQL cooling–lubrication methods. The residual stresses were measured at depths of 0, 10, 30, 50, 100, and 150 µm below the surface in accordance with the EN 15305:2008 standard [26]. X-ray diffraction (XRD) measurements were performed using a chromium (Cr) X-ray source. The diffraction peak at a Bragg angle of 156.4° was used, with a collimator (2 mm) and a collimator spacing of 9.85 mm. The Cr tube was operated at 30 kV and 9 mA. The measurements were performed with sin2 ψ in modified χ-mode. Young's modulus of 211 MPa and Poisson's ratio of 0.3 were used for the reflection. The full width at half maximum (FWHM) was determined using the cross-correlation peak fitting method.

Microhardness was measured using a Wilson Instruments Tukon 2100B (Instron, USA) Vickers hardness tester in accordance with ISO 6507-1:2018 standard [27]. The load used for the measurements was 50 g. Measurements were taken at a depth ranging from 0 µm to 500 µm from the surface.

## 3. Results and Discussions

In order to evaluate the efficiency of the two studied cooling–lubrication methods ($LCO_2$ + MQL and flood cooling), it is necessary to distinguish between their respective lubrication and cooling capabilities. Lubrication effectiveness was assessed based on grinding forces, specific energy, and the force ratio. These grindability indicators provide insight into the friction and energy balance within the grinding zone. On the other hand, cooling effectiveness pertains to the efficacy of the methods in removing heat from the grinding zone. This directly impacts the grinding temperature, which can potentially lead to thermal damage, such as softening (a reduction in work material hardness) and the onset of residual tensile stresses. The grindability was therefore evaluated by measuring the grinding forces, calculating the specific grinding energy and force ratios, and assessing the surface integrity through measurements of surface roughness, residual stresses, and microhardness.

### *3.1. Grinding Forces*

The grinding forces are directly related to the grinding performance, grinding parameters, energy consumption, dressing procedure, and the cooling–lubrication methods used [28]. As noted earlier, the tangential ($F_t$) and normal ($F_n$) components of the grinding forces were measured for different grinding conditions (refer to Table 2) under both flood cooling and $LCO_2$ + MQL. The measured grinding force represents the total forces exerted by the active grits on the workpiece.

Figure 3a,b show the variation in normal and tangential forces in relation to different *Aggr*. The normal grinding forces in $LCO_2$ + MQL grinding ranged from 13.5 N to 166.7 N, while in flood grinding conditions, they ranged from 7.3 N to 124.3 N. Additionally, the tangential grinding forces in $LCO_2$ + MQL grinding ranged from 3.3 N to 74.3 N, and in flood grinding, they ranged from 3.7 N to 59.5 N. Under higher aggressiveness conditions, both the normal and tangential grinding forces were found to be larger in $LCO_2$ + MQL grinding than in flood grinding. This may be due to the inability of the gaseous $LCO_2$ + MQL to effectively break the air barrier around the grinding wheel periphery and penetrate the grinding zone. Furthermore, the frozen oil layer generated by $LCO_2$ + MQL may exacerbate the issue by obstructing the coolant-lubricant flow, further increasing the grinding forces [29].

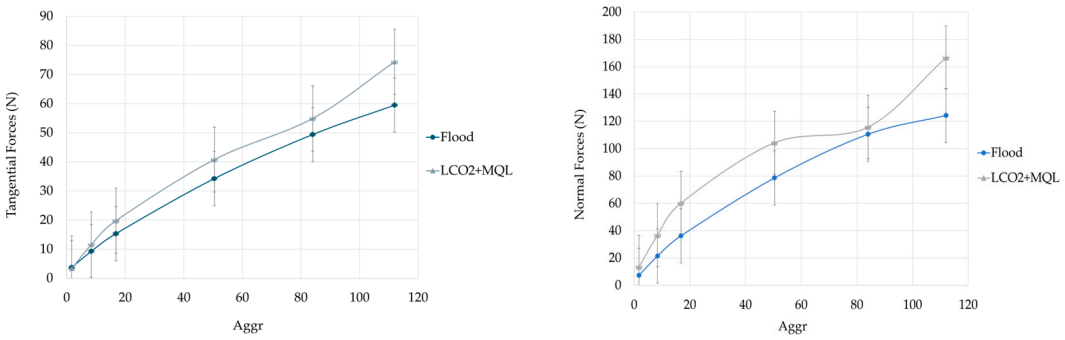


(**a**) (**b**)

**Figure 3.** (**a**) Normal grinding forces vs. *Aggr*; (**b**) tangential forces vs. *Aggr*.

The measured tangential force component was used to calculate the specific grinding energy, which is the amount of energy required to remove a unit volume of material. The latter parameter is a crucial parameter for evaluating the grinding process efficiency and is a widely used grindability metric [30,31]. It can be calculated as follows [2]:

$$e_c = \frac{F_t \times V_s}{V_w \times a_e \times b_D} \quad (2)$$

where $b_D$ is the grinding width.

Figure 4 shows the specific energy versus *Aggr* for the flood and $LCO_2$ + MQL grinding conditions. The specific energy at lower *Aggr* is higher due to higher sliding and plowing energies, a phenomenon known as the size effect [32]. Flood cooling results in the highest specific energy (112.1 J/mm$^3$) at the lowest *Aggr*, but at higher *Aggr*, it exhibits the lowest specific energy of 26.9 J/mm$^3$, which falls within the typical range for the production grinding of steels, generally between 30 and 60 J/mm$^3$. The obtained specific energy curves depend on the tangential grinding forces, and the higher tangential forces observed with $LCO_2$ + MQL compared to flood cooling suggest that $LCO_2$ + MQL may provide insufficient lubrication. The increased normal forces also result in higher contact pressure, which could indirectly lead to higher specific energy. According to Malkin [33], lubrication decreases both the cutting energy (expanded for plowing and chip formation) and the sliding energy in grinding (by reducing attritious wear). Although no-dress tests were not performed in this study to observe the wear flat formation, additional insights can be gained by analyzing the force ratio.

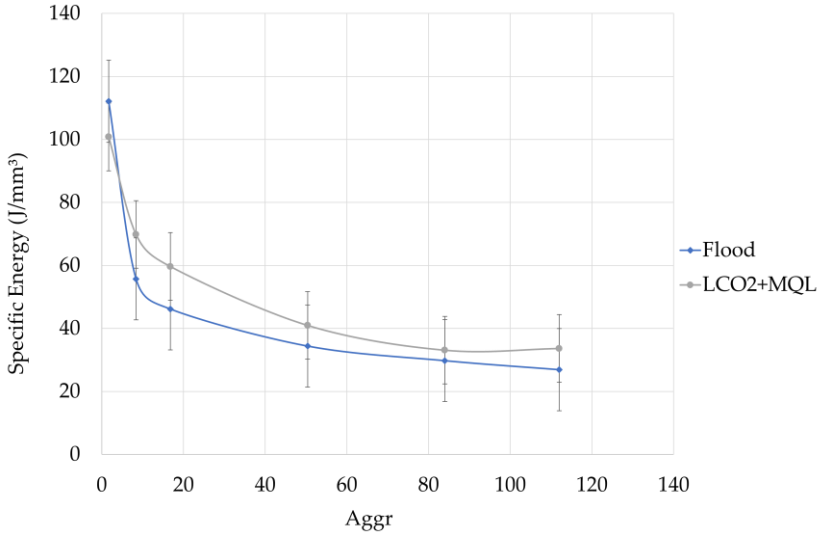


**Figure 4.** Specific energy vs. *Aggr*.

The grinding force ratio ($F_t/F_n$) can be interpreted as an indicator of the balance between the cutting forces and sliding forces within the grinding zone [33]. Figure 5 shows the variation in the force ratio as a function of *Aggr* for both flood cooling and $LCO_2$ + MQL grinding conditions. At lower *Aggr* values, $LCO_2$ + MQL grinding yielded a much lower force ratio of 0.24 compared to flood cooling, which exhibited a significantly higher ratio of 0.51. This indicates that under low *Aggr* conditions, the normal force in $LCO_2$ + MQL is about four times larger than the tangential force. In contrast, with flood cooling, the normal force is only about twice as large, implying more efficient cutting with less sliding. As the grinding aggressiveness increased, the force ratio for $LCO_2$ + MQL also increased, reaching 0.44 at the highest *Aggr*, while flood cooling remained relatively stable at 0.47. The rise in force ratio for $LCO_2$ + MQL with increasing *Aggr* reflects a shift from sliding to more efficient chip formation as cutting becomes more dominant. However, the force ratio for $LCO_2$ + MQL remained lower than for flood cooling, where consistent lubrication allowed for a more balanced force distribution.

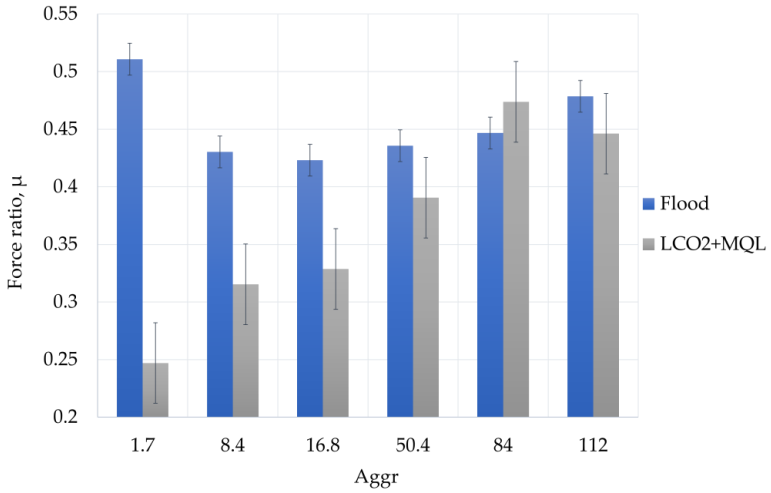


**Figure 5.** Force ratio vs. *Aggr* for different grinding conditions.

### *3.2. Surface Roughness*

Given that lubrication improves the surface finish of ground workpieces, the arithmetic mean height roughness ($R_a$) was measured to further determine which method provides better lubrication. Figure 6 illustrates the relationship between $R_a$ and different *Aggr* under the two studied cooling–lubrication conditions. The results indicate that the surface roughness is lower at the lowest *Aggr* for both cooling–lubrication methods, which was expected. This occurs because the grits of the grinding wheel penetrate less deep into the workpiece at lower aggressiveness, and because in surface grinding, the surface roughness increases with $\frac{V_w}{V_s}$, especially when the depth of cut is constant. The average $R_a$ value for $LCO_2$ + MQL was 0.38 μm at the lowest *Aggr*, while for flood cooling, it was 0.44 μm. This finding is important, as grinding is typically employed for the final finishing of components (i.e., grinding with low *Aggr*). At the highest *Aggr* tested, the obtained surface finish is nearly the same—flood cooling results in an average $R_a$ of 0.80 μm, while $LCO_2$ + MQL results in an average $R_a$ of 0.82 μm. The dependence of surface roughness on grit sharpness and grit fracture has been reported in several studies. The retention of grit sharpness can be achieved by cryogenic cooling [29,34–39] and the formation of boundary lubrication by MQL [40] may be responsible for a comparable surface finish.

Under all tested conditions, $LCO_2$ + MQL achieved surface roughness values comparable to those of flood cooling. One should note also that the relatively large variation in $R_a$ measurements makes it difficult to draw definitive conclusions about the superiority of either cooling–lubrication method in terms of providing a smoother surface finish.

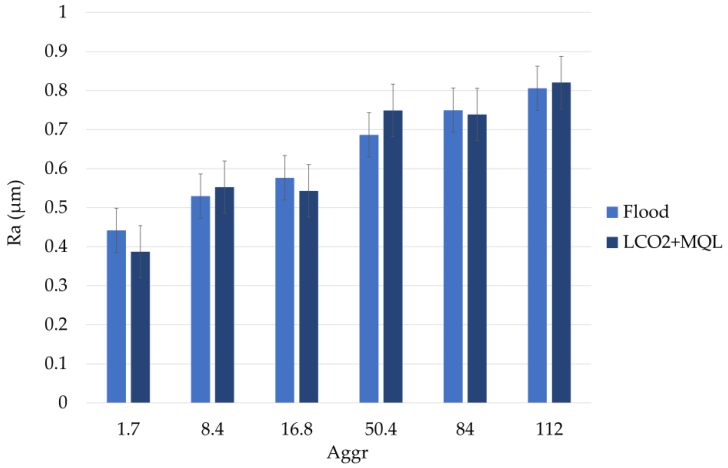


**Figure 6.** Arithmetic mean height roughness ($R_a$) vs. *Aggr*.

### 3.3. Residual Stresses

In grinding, temperatures and the energy partition to the workpiece are key indicators of cooling effectiveness. However, since direct temperature measurements were not taken in this study, the most reliable indirect method of assessing cooling efficiency is through the evaluation of residual stresses. Figure 7 illustrates the residual stress profiles in transverse and longitudinal directions relative to the grinding direction for the different cooling–lubrication methods used. It can be observed that the surface residual stresses in both directions tend to be tensile at higher *Aggr* and compressive at lower *Aggr*. These results are logical, as grinding at higher *Aggr* is associated with higher temperatures, which can lead to thermally induced tensile stresses. However, at lower *Aggr*, thermal loads are reduced, and the residual compressive stresses are primarily caused by mechanical action between the grits and the workpiece.

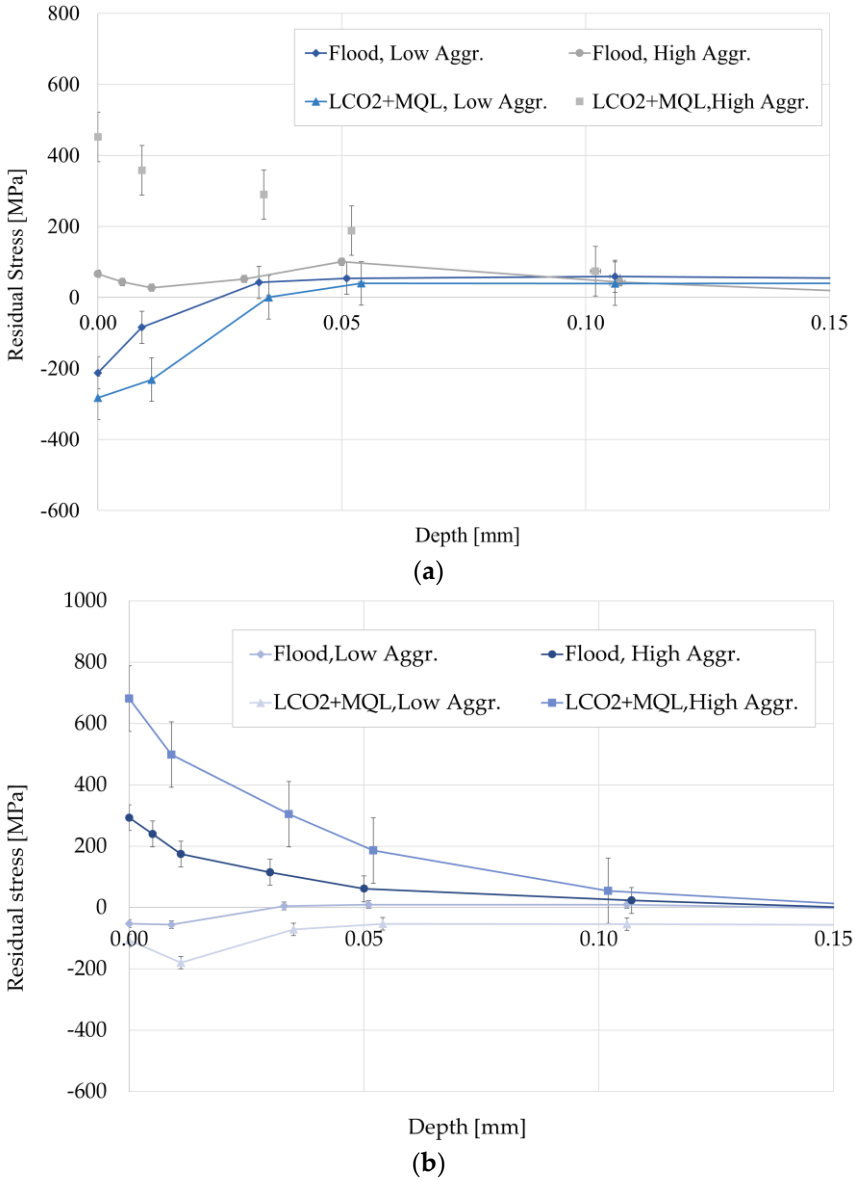


**Figure 7.** Grinding-induced residual stress profiles measured in (**a**) transverse direction, (**b**) longitudinal direction.

In the transverse direction, $LCO_2$ + MQL exhibits a maximum tensile residual stress of 451.9 MPa and the flood cooling has a value of 66.7 MPa at higher aggressiveness on the ground surface. In the longitudinal direction, the maximum tensile residual stress is

681.2 MPa for $LCO_2$ + MQL and 293 MPa for flood cooling on the ground surface. These observations align with previous research, suggesting that residual tensile stresses along the grinding direction are predominant [2]. The highest surface compressive stresses were found for $LCO_2$ + MQL grinding at the lowest *Aggr*, i.e., in the transverse direction with a value of—282.9 MPa and in the longitudinal direction with a value of −106.9 MPa.

At lower *Aggr*, grinding with $LCO_2$ + MQL results in higher compressive stresses; this is likely because heat is dissipated more effectively and also due to mechanical action, as material removal is mostly due to shearing and plowing effects rather than sliding [41]. This suggests that the combination of low *Aggr* and a potentially larger area of successful heat evacuation around the grinding zone, facilitated by the vaporization and expansion of $LCO_2$ upon exiting the nozzle, helped to prevent the onset of thermally induced residual tensile stresses. When $LCO_2$ is employed, several critical effects may come into play, influencing the resulting residual stresses. As the grinding zone and its vicinity are exposed to lower temperatures due to the $LCO_2$ environment, the thermal expansion of the hotter material near the surface becomes less pronounced. This likely mitigates the constraint on expansion, allowing the material to experience reduced thermal expansion, which can contribute to a more favorable stress distribution. Here, it should be clarified that upon exiting the nozzle, $LCO_2$ vaporizes and expands, absorbing heat from the surroundings through mechanisms such as evaporation, Joule–Thompson cooling, and sublimation [42]. This exposes not only the immediate grinding zone but also a larger area around the workpiece to lower temperatures. The temperature in this region reaches −78.5 °C (194.65 K), the boiling point of $CO_2$, facilitating heat evacuation and reducing the onset of residual tensile stresses. Beyond a depth of 0.05 mm, both compressive and tensile residual stress start to decrease.

The formation of residual tensile stresses at higher *Aggr* is due to higher heat generation in the grinding zone, which causes thermal stress [43]. $LCO_2$ + MQL grinding exhibits higher residual tensile stresses at higher *Aggr* than flood grinding, owing to the limitations in heat dissipation due to the rapid evaporation of $LCO_2$. While the MWF in flood cooling is in a liquid form, allowing it to stay in contact with the workpiece surface for a longer duration and continuously evacuate heat, $LCO_2$, which transitions to a gaseous state upon exiting the nozzle, may not be as effective in maintaining contact with the workpiece surface and removing heat. This prolonged contact in flood cooling improves its heat dissipation capabilities at higher *Aggr*, whereas $LCO_2$ + MQL struggles to dissipate heat as effectively in these conditions. Hence, $LCO_2$ + MQL grinding at high *Aggr* reveals worse results (higher tensile stresses).

To further characterize the ground subsurface, the FWHM (full width at half maximum) values at the lowest and highest *Aggr* for flood cooling and $LCO_2$ + MQL cooling are plotted in Figure 8. The FWHM values are related to various surface distortions caused by the grinding process [44]. The FWHM values are higher for $LCO_2$ + MQL in both the transverse and longitudinal directions compared to flood cooling. In both directions, the FWHM values range from 1.9° to 3.1°. The higher FWHM values at the surface are likely due to plastic deformation causing crystal lattice distortions, leading to the broadening of the diffraction peaks caused by the rubbing of the wheel on the surface [45]. As reported by Pušavec et al. [45], the FWHM values are related to the plastic work, which depends on the mechanical loadings, whereas residual stress depends on both mechanical and thermal effects. Even though $LCO_2$ + MQL has higher tensile residual stresses compared to flood cooling, higher FWHM values indicate a higher amount of plastic work in the case of $LCO_2$ + MQL grinding process. This is logical, as the lower force ratio in $LCO_2$ + MQL grinding means more plowing and less efficient chip formation, contributing to greater plastic deformation.

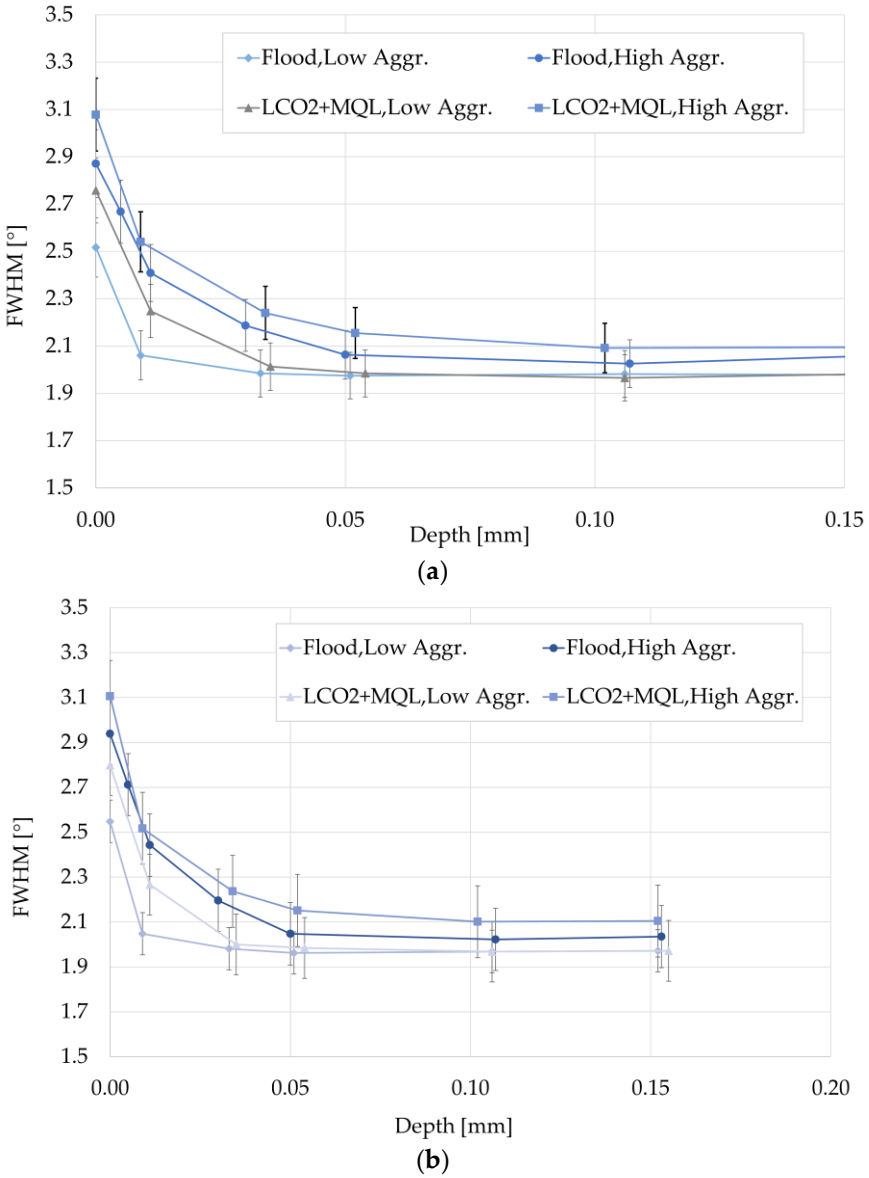


**Figure 8.** (**a**) FWHM values (transverse) direction; (**b**) FWHM values (longitudinal) direction.

### *3.4. Microhardness Measurements*

Microhardness profiles were measured for the lowest and highest *Aggr* values for the different grinding conditions, as shown in Figure 9. The resulting microhardness across various depths maintained a consistent level of approximately 350 HV for all conditions, indicating no significant difference in microhardness between flood and $LCO_2$ + MQL grinding. This consistency suggests that the cooling–lubrication method does not significantly influence the subsurface hardness of the material. The highest microhardness values were observed between depths of 200 µm and 400 µm. Under the highest *Aggr* conditions, flood grinding exhibited a microhardness of 349 $HV_{0.05}$, while $LCO_2$ + MQL grinding showed a value of 346 $HV_{0.05}$. Conversely, at the lowest *Aggr* conditions, flood grinding recorded a microhardness of 331 HV0.05, and $LCO_2$ + MQL showed a value of 349 $HV_{0.05}$.

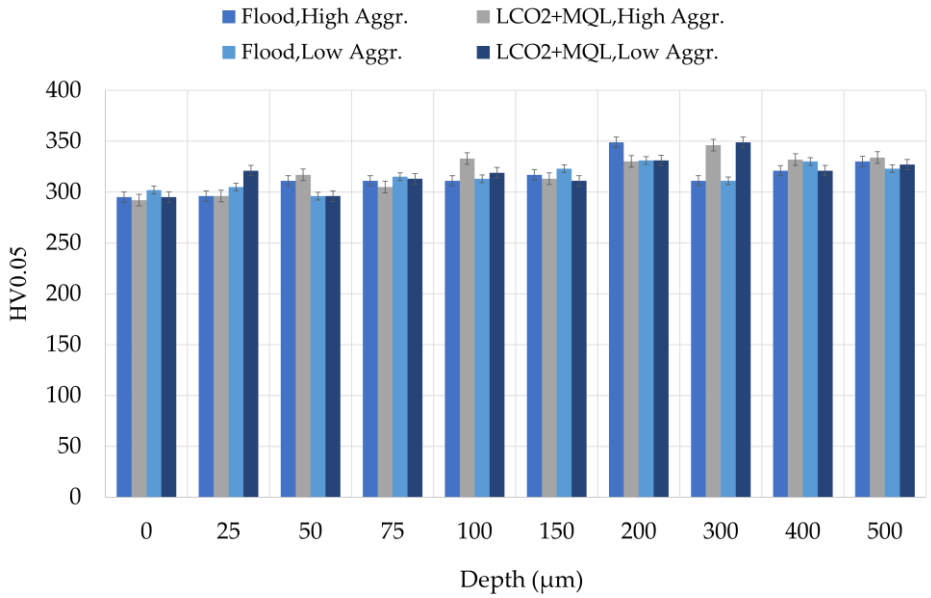


**Figure 9.** Microhardness vs. depth beneath surface for different grinding conditions.

A slight reduction in hardness was observed on the surface of the workpiece up to a depth of 50 μm, likely due to the influence of grinding temperature, which causes the tempering of martensite that leads to a slight decrease in hardness [46]. Both cooling–lubrication methods appear to effectively mitigate the thermal softening typically caused by the heat generated during grinding.

### *3.5. Cost-Effectiveness Analysis*

Following the detailed assessment of the technological viability of $LCO_2$ + MQL in terms of grindability, a supplementary cost-effectiveness analysis (CEA) will be conducted to assess its economic feasibility in comparison to conventional flood cooling. Conventional flood cooling remains the most widely used method in industrial grinding due to its practical advantages, such as cleaning the grinding wheel during the process (reducing clogging), effectively flushing chips from the machine's work area, and the ability to install large central MWF reservoirs that serve multiple machine tools simultaneously. These benefits, coupled with the perception of lower operating costs, make it the standard choice for most end users. Based on the CEA presented below, the preliminary results show that the alternative cooling–lubrication method using $LCO_2$ + MQL is not only technically feasible and provides comparable grindability results but is also comparable in terms of cost.

For a single machine tool used in this study, the total annual cost of $LCO_2$ + MQL, including equipment depreciation over 5 years, is 41,580 EUR/year (Table 3). In comparison, the cost of conventional flood cooling is 42,329 EUR/year (Table 4). The CEA assumes that the machine operates three shifts per day, with an overage operational time of 20.4 h per day (at an Overall Equipment Effectiveness (OEE) of 85%), and runs for 250 days per year. This analysis shows that even on the level of a single machine (with a 1400 L reservoir), conventional flood cooling can incur significant costs due to the need to replenish lost grinding fluid (Table 4). In real-world production scenarios, these costs are magnified. For example, in large industrial environments such as automotive (engine, transmission) plants, a central MWF system for a grinding production line may hold up to 100,000 L of water-based MWF and experience a 10% daily fluid loss due to high temperatures, evaporation and ventilation requirements (to keep aerosol levels on the shopfloor below regulatory thresholds). In contrast, the $LCO_2$ + MQL system benefits from a more controlled and efficient use of resources, as $LCO_2$ + MQL can be precisely applied only when the grinding wheel is engaged, minimizing consumption during non-cutting phases ("air grinding").

In addition, the $LCO_2$ used was sourced as "green $CO_2$"—captured as a by-product of bioethanol production. Such recycled $CO_2$ does not add additional greenhouse gasses to the atmosphere, making the environmental impact of $LCO_2$ + MQL much lower in terms of $CO_2$ emissions. In addition, the $LCO_2$ + MQL system completely eliminates the need for (i) the cleaning of components after grinding, and (ii) water—reducing costs associated with water consumption and wastewater management challenges.

**Table 3.** Cost analysis: $LCO_2$ + MQL method.

| Inputs | Value | Outputs | Value |
|---|---|---|---|
| Mass flow rate of $CO_2$ | 170 g/min | Consumption of $CO_2$ | 26,010 kg/year |
| Cost of $CO_2$ | 1 EUR/kg | Annual cost of $CO_2$ | 26,010 EUR/year |
| MQL flow rate | 35 mL/h | Annual MQL consumption | 179 L/year |
| Cost of MQL oil | 20 EUR/L | Annual cost of MQL oil | 3570 EUR/year |
| Utilization of $LCO_2$-MQL | 50% | | |
| $LCO_2$-MQL equipment investment | 60,000 EUR | | |
| Equipment cost (5-year depreciation) | 12,000 EUR/year | | |
| Total for $LCO_2$-MQL→41,580 EUR/year | | | |

**Table 4.** Cost analysis: conventional flood cooling.

| Inputs | Value | Outputs | Value |
|---|---|---|---|
| Grinding fluid volume | 1400 L | Daily MWF loss | 140 L/day |
| Solution concentration | 8% | Annual MWF loss | 35,000 L/year |
| Cost of grinding fluid | 15 EUR/L | Volume of MWF loss | 2800 L/year |
| Cost of water | 1.7 EUR/1000 L | Volume of water lost | 32,200 L/year |
| Electricity cost | 0.03 EUR/kWh | Cost of lost MWF | 42,000 EUR/year |
| Daily MWF loss | 10% | Cost of lost water | 55 EUR/year |
| Pump power | 1.3 kW | Annual energy use (pump) | 6630 kWh |
| Electricity emissions factor | 0.09 kg $CO_2$/kWh | Pump energy cost | 199 EUR/year |
| $CO_2$ emission cost | 122 EUR/ton | $CO_2$ emissions from electricity | 597 kg $CO_2$/year |
| | | Annual $CO_2$ emission cost | 73 EUR/year |
| | | Water cost for conventional cooling | 57 EUR/year |
| Total for flood cooling→42,329 EUR/year | | | |

While the $LCO_2$ + MQL system demonstrates comparable cost and more favorable environmental benefits for a single machine tool, these impacts may not be directly scalable to larger production lines. In an 8–10 machine tool/line scenario, the cost of implementing $LCO_2$ + MQL could increase due to the need for either more single $LCO_2$ + MQL units or the development of a more complex centralized system capable of serving multiple machines. Scaling such a system would require additional ancillary equipment, including larger $CO_2$ storage tanks, distribution infrastructure, and controllers. This additional infrastructure could reduce the overall cost parity observed at the single machine level, making scaling $LCO_2$ + MQL more challenging and potentially more expensive. However, as the industry is increasingly shifting towards fossil-free production, environmental regulations tighten, and the costs of water treatment and hazardous waste disposal from conventional flood cooling increase, the long-term advantages of $LCO_2$ + MQL may become more pronounced. Future technological advances could further reduce the cost of $LCO_2$ + MQL equipment, making it an even more attractive option for wider applications. It is important to note here, however, that this is not a comprehensive cost–benefit analysis, but a simplified comparative analysis to highlight major costs associated with both systems. A more formal analysis would need to be incorporated into a Life Cycle Assessment (LCA) framework to capture broader sustainability impacts, such as Scope 1, 2, and 3 emissions. In the case of conventional metalworking fluids (MWFs), as much as 96% of the associated emissions are

indirect (Scope 3), resulting from activities such as the procurement of raw materials. While the methodology for calculating Product Carbon Footprints (PCFs) for MWFs is available, a full analysis is beyond the scope of this work. The main objective of this work is to investigate the technical feasibility of implementing $LCO_2$ + MQL as a cooling–lubrication method in an industrial grinding machine tool.

## 4. Conclusions

Due to the limited investigations of the $LCO_2$ + MQL cooling–lubrication method in grinding, this study focused on evaluating its effects on the grindability of AISI 4140 steel. Comparisons were made against conventional flood cooling across key grindability indicators, including grinding forces, specific energy, force ratio, surface roughness, residual stresses, and microhardness profiles. The findings lead to the following conclusions:

- The normal grinding forces were 25% higher, tangential normal forces were 20% higher, and specific energies were 10–20% higher for $LCO_2$ + MQL grinding at higher *Aggr* values. This increase can primarily be attributed to the inefficient cooling capability of $LCO_2$ + MQL during rough grinding, likely due to the limited cooling capability of $LCO_2$ + MQL, as the gaseous $LCO_2$ is less effective at maintaining contact with the workpiece and evacuating heat, unlike the liquid MWF in flood cooling, which remains in contact longer and improves heat dissipation.
- The force ratio was significantly lower for $LCO_2$ + MQL at lower *Aggr*, indicating insufficient lubrication. As *Aggr* increased, the force ratio for $LCO_2$ + MQL improved, but it remained consistently lower than that of flood cooling, which provided better lubrication across all conditions.
- The study found that the average surface roughness achieved with $LCO_2$ + MQL was comparable to that achieved with conventional flood cooling.
- Both cooling–lubrication methods resulted in residual tensile stresses at higher *Aggr* (rough grinding) and residual compressive stresses at lower *Aggr* (finish grinding). $LCO_2$ + MQL induced more pronounced residual tensile stresses at higher *Aggr*, while at lower *Aggr*, more favorable residual stresses were observed. The analysis of the full width at half maximum (FWHM) profiles indicated higher values for $LCO_2$ + MQL at higher *Aggr*, suggesting greater plastic deformation. At lower *Aggr*, $LCO_2$ + MQL exhibited comparable FWHM results to flood cooling, likely due to the mechanical effects dominating over thermal ones.
- Microhardness measurements revealed negligible differences between the $LCO_2$ + MQL and flood cooling, indicating similar effects on the workpiece subsurface. $LCO_2$ + MQL proved effective in preventing the tempering (softening) of the work material under all of the grinding conditions tested.
- The preliminary cost-effectiveness analysis suggests that $LCO_2$ + MQL is not only technologically feasible in terms of delivering comparable grindability results, but also demonstrates cost effectiveness.

While previous studies have often demonstrated that MQL, sometimes combined with cryogenic coolant, generally outperforms conventional flood cooling in terms of reducing specific energy, achieving smoother surface finishes, and improving the G-ratio, this was not observed in the present study. The likely reason is that the nozzle configuration was not optimized, and further investigation is needed to determine if gaseous $LCO_2$ + MQL can penetrate the air barrier around the wheel periphery. Moreover, without investigating wheel wear progression (e.g., attritious dulling of the grits), it was not possible to fully evaluate how $LCO_2$ + MQL impacts chip formation and plowing energies during grinding. Additionally, to better investigate the cooling capabilities of $LCO_2$ + MQL, temperature measurements should be considered in future work.

**Author Contributions:** Conceptualization, P.K., P.H., and D.K.S.; methodology, P.H. and D.K.S. software, validation, P.H. and D.K.S.; formal analysis, P.K.; writing—original draft preparation,

D.K.S.; writing—review and editing, P.K., F.P., and P.H. All authors have read and agreed to the published version of the manuscript.

**Funding:** This work was supported by the Slovenian Research Agency under Grant: L2-50079: Research on near-dry cryogenic shearing to achieve cleaner production with less waste in the serial automotive industry and P2-0266: Advanced manufacturing technologies for high-quality and sustainable production and partially supported by the EIT Manufacturing Programme under the project Transitioning to a Waste-free Production—International Cryogenic + MQL Machining Activity (number - 21193).

**Data Availability Statement:** The datasets presented in this study are available on request from the corresponding author; they are not publicly available as they form part of ongoing research.

**Acknowledgments:** The authors would like to thank Jonas Holmberg, Research Institutes of Sweden (RISE), for their help with the residual stress measurements and Borut Žužek, Institute of Metals and Technology, Slovenia, for their help with the microhardness measurements.

**Conflicts of Interest:** The authors declare no conflicts of interest.

## References

1. Chen, S.; Yang, S.; Cheung, C.F.; Liu, T.; Duan, D.; Ho, L.T.; Jiang, Z. Study on the Surface Generation Mechanism during Ultra-Precision Parallel Grinding of SiC Ceramics. *Crystals* **2023**, *13*, 646. [CrossRef]
2. Malkin, S.; Guo, C. *Grinding Technology: Theory and Application of Machining with Abrasives*, 2nd ed.; Industrial Press Inc.: New York, NY, USA, 2008.
3. Kishore, K.; Sinha, M.K.; Singh, A.; Archana; Gupta, M.K.; Korkmaz, M.E. A Comprehensive Review on the Grinding Process: Advancements, Applications and Challenges. *Proc. Inst. Mech. Eng. C J. Mech. Eng. Sci.* **2022**, *236*, 10923–10952. [CrossRef]
4. Heep, T.; Bickert, C.; Abele, E. Application of Carbon Dioxide Snow in Machining of CGI Using an Additively Manufactured Turning Tool. *J. Manuf. Mater. Process.* **2019**, *3*, 15. [CrossRef]
5. Kishawy, H.A.; Hegab, H.; Deiab, I.; Eltaggaz, A. Sustainability Assessment during Machining Ti-6Al-4V with Nano-Additives-Based Minimum Quantity Lubrication. *J. Manuf. Mater. Process.* **2019**, *3*, 61. [CrossRef]
6. Qian, N.; Chen, J.; Khan, A.M.; Zhao, B.; Chen, Y.; Ding, W.; Fu, Y.; Xu, J. Towards Sustainable Grinding of Difficult-to-Cut Alloys—A Holistic Review and Trends. *Chin. J. Mech. Eng.* **2024**, *37*, 23. [CrossRef]
7. Liang, C.; Gong, Y.; Zhou, L.; Qi, Y.; Zhang, H.; Zhao, J. Tool Wear Mechanism and Grinding Performance for Different Cooling-Lubrication Modes in Grinding of Nickel-Based Superalloys. *Materials* **2023**, *16*, 3545. [CrossRef]
8. Patil, A.S.; Sunnapwar, V.K.; S. Bhole, K.; Ray, M.P.; More, Y.S. Effective Cooling Methods for Ti6Al4V CNC Milling: A Review. *Adv. Mater. Process. Technol.* **2023**, *9*, 457–506. [CrossRef]
9. Hanenkamp, N.; Amon, S.; Gross, D. Hybrid Supply System for Conventional and $CO_2$/MQL-Based Cryogenic Cooling. *Procedia CIRP* **2018**, *77*, 219–222. [CrossRef]
10. García, E.; Méresse, D.; Pombo, I.; Dubar, M.; Sánchez, J.A. Role of Frozen Lubricant Film on Tribological Behaviour and Wear Mechanisms in Grinding. *Int. J. Adv. Manuf. Technol.* **2016**, *82*, 1017–1027. [CrossRef]
11. Mahata, S.; Mukhopadhyay, M.; Kundu, A.; Banerjee, A.; Mandal, B.; Das, S. Grinding Titanium Alloys Applying Small Quantity Lubrication. *SN Appl. Sci.* **2020**, *2*, 978. [CrossRef]
12. Arafat, R.; Madanchi, N.; Thiede, S.; Herrmann, C.; Skerlos, S.J. Supercritical Carbon Dioxide and Minimum Quantity Lubrication in Pendular Surface Grinding—A Feasibility Study. *J. Clean Prod.* **2021**, *296*, 126560. [CrossRef]
13. Liu, M.; Li, C.; Yang, M.; Gao, T.; Wang, X.; Cui, X.; Zhang, Y.; Said, Z.; Sharma, S. Mechanism and enhanced grindability of cryogenic air combined with biolubricant grinding titanium alloy. *Tribol. Int.* **2023**, *187*, 108704. [CrossRef]
14. Balan, A.S.; Vijayaraghavan, L.; Krishnamurthy, R.; Kuppan, P.; Oyyaravelu, R. An experimental assessment on the performance of different lubrication techniques in grinding of Inconel 751. *J. Adv. Res.* **2016**, *7*, 709–718. [CrossRef] [PubMed]
15. Sharma, A.; Chaudhari, A.; Diwakar, V.; Awale, A.S.; Yusufzai, M.Z.; Vashista, M. Implementation of hybrid CryoMQL sustainable lubri-cooling to enhance the grindability and surface integrity of tool steel. *J. Manuf. Process.* **2024**, *119*, 16–31. [CrossRef]
16. Bergs, T.; Pusavec, F.; Koch, M.; Grguras, D.; Dobbeler, B.; Klocke, F. Investigation of the Solubility of Liquid $CO_2$ and Liquid Oil to Realize an Internal Single Channel Supply in Milling of Ti6Al4V. *Procedia Manuf.* **2019**, *33*, 200–207. [CrossRef]
17. Grguraš, D.; Sterle, L.; Krajnik, P.; Pušavec, F. A Novel Cryogenic Machining Concept Based on a Lubricated Liquid Carbon Dioxide. *Int. J. Mach. Tools Manuf.* **2019**, *145*, 103456. [CrossRef]
18. Santhosh, K.; Pušavec, F.; Krajnik, P. Grinding of Cemented Carbide Using a Vitrified Diamond Pin and Lubricated Liquid Carbon Dioxide. *Stroj. Vestn.-J. Mech. Eng.* **2023**, *69*, 435–443. [CrossRef]
19. Ruiz-Trabolsi, P.A.; Chino-Ulloa, A.; Miranda-Hernández, J.G.; Tadeo-Rosas, R.; Carrera-Espinoza, R.; Velázquez, J.C.; Hernández-Sánchez, E. A Comparative Analysis of the Tribological Behavior of Hard Layers Obtained by Three Different Hardened-Surface Processes on the Surface of AISI 4140 Steel. *Crystals* **2022**, *12*, 298. [CrossRef]

20. Özdemir, M.; Şahinoğlu, A.; Rafighi, M.; Yilmaz, V. Analysis and optimisation of the cutting parameters based on machinability factors in turning AISI 4140 steel. *Can. Metall. Q.* **2022**, *61*, 407–417. [CrossRef]
21. Kohls, E.; Heinzel, C.; Eich, M. Evaluation of Hardness and Residual Stress Changes of AISI 4140 Steel Due to Thermal Load during Surface Grinding. *J. Manuf. Mater. Process.* **2021**, *5*, 73. [CrossRef]
22. Grguraš, D.F.; Sterle, L.; Malneršič, A.; Kastelic, L.; Courbon, C.; Pušavec, F. Media Flow Analysis of Single-Channel Pre-Mixed Liquid $CO_2$ and MQL in Sustainable Machining. *Stroj. Vestn.-J. Mech. Eng.* **2021**, *67*, 3–11.
23. Drazumeric, R.; Badger, J.; Krajnik, P.; Kopac, J. Thermal Aspects and Grinding Aggressiveness in View of Optimizing High-Performance Grinding Operations in the Automotive Industry. In Proceedings of the International Manufacturing Science and Engineering Conference Detroit, Detroit, MI, USA, 9–13 June 2014; Volume 2.
24. ISO 4287:1997 Geometrical Product Specifications (GPS) - Surface Texture: Profile Method - Terms, Definitions and Surface Texture Parameters. Available online: https://www.iso.org/standard/44475.html (accessed on 12 October 2024).
25. BS EN ISO 21920-2:2022 - Geometrical Product Specifications (GPS). Surface Texture: Profile Terms, Definitions and Surface Texture Parameters. Available online: https://www.iso.org/obp/ui/#iso:std:iso:21920:-2:ed-1:v2:en (accessed on 12 October 2024).
26. ISO 6507-1:2018-Metallic Materials-Vickers Hardness Test-Part 1: Test Method. Available online: https://www.en-standard.eu/iso-6507-1-2018-metallic-materials-vickers-hardness-test-part-1-test-method/ (accessed on 12 October 2024).
27. BS EN 15305:2008 Non-Destructive Testing. Test Method for Residual Stress Analysis by X-ray Diffraction. Available online: https://knowledge.bsigroup.com/products/non-destructive-testing-test-method-for-residual-stress-analysis-by-x-ray-diffraction?version=standard. (accessed on 12 October 2024).
28. Liu, M.; Li, C.H.; An, Q.; Zhang, Y.; Yang, M.; Cui, X.; Gao, T.; Dambatta, Y.S.; Li, R. Atomized Droplets Liquid Film Thickness Model and Verification in Sustainable Hybrid Lubrication (Cryo-Mql) Grinding. *SSRN* **2024**. [CrossRef]
29. Sanchez, J.A.; Pombo, I.; Alberdi, R.; Izquierdo, B.; Ortega, N.; Plaza, S.; Martinez-Toledano, J. Machining Evaluation of a Hybrid MQL-$CO_2$ Grinding Technology. *J. Clean Prod.* **2010**, *18*, 1840–1849. [CrossRef]
30. Hoier, P.; Azarhoushang, B.; Lundin, P.; Malakizadi, A.; Badger, J.; Stormvinter, A.; Björk, T.; Klement, U.; Hashimoto, F.; Krajnik, P. Influence of batch-to-batch material variations on grindability of a medium-carbon steel. *J. Manuf. Process.* **2022**, *73*, 463–470. [CrossRef]
31. Hoier, P.; Kareepadath Santhosh, D.; Hryha, E.; Krajnik, P. An investigation into the grindability of additively manufactured 42CrMo4 steel. *CIRP Ann.* **2024**, *73*, 257–260. [CrossRef]
32. Ding, W.; Xu, J.; Chen, Z.; Su, H.; Fu, Y. Grindability and Surface Integrity of Cast Nickel-Based Superalloy in Creep Feed Grinding with Brazed CBN Abrasive Wheels. *Chin. J. Aeronaut.* **2010**, *23*, 501–510.
33. Osman, M.; Malkin, S. Lubrication by Grinding Fluids at Normal and High Wheel Speeds. *A S L E Trans.* **1972**, *15*, 261–268. [CrossRef]
34. Mao, C.; Zhang, J.; Huang, Y.; Zou, H.; Huang, X.; Zhou, Z. Investigation on the Effect of Nanofluid Parameters on MQL Grinding. *Mater. Manuf. Process.* **2013**, *28*, 436–442. [CrossRef]
35. Singh, P.K.; Kumar, S.; Jain, P.K. Effect of Cryogenic Grinding on Surface Characteristics of Additively Manufactured Ti-6Al-4V Alloy. *Surf. Topogr. Metrol. Prop.* **2023**, *11*, 015014. [CrossRef]
36. Li, C.H.; Lu, B.H.; Ding, Y.C.; Cai, G.Q. Innovative Technology Investigation into Cryogenic Cooling Green Grinding Using Liquid Nitrogen Jet. In Proceedings of the 2009 International Conference on Management and Service Science, Beijing, China, 20–22 September 2009.
37. Manimaran, G.; Pradeep kumar, M.; Venkatasamy, R. Surface Modifications in Grinding AISI D3 Steel Using Cryogenic Cooling. *J. Braz. Soc. Mech. Sci. Eng.* **2015**, *37*, 1357–1363. [CrossRef]
38. Setti, D.; Yadav, N.K.; Ghosh, S. Grindability Improvement of Ti-6Al-4V Using Cryogenic Cooling. *Proc. Inst. Mech. Eng. B J. Eng. Manuf.* **2014**, *228*, 1131–1137. [CrossRef]
39. Balan, A.S.S.; Chidambaram, K.; Kumar, A.V.; Krishnaswamy, H.; Pimenov, D.Y.; Giasin, K.; Nadolny, K. Effect of Cryogenic Grinding on Fatigue Life of Additively Manufactured Maraging Steel. *Materials* **2021**, *14*, 1245. [CrossRef] [PubMed]
40. Yaqoob, S.; Ghani, J.A.; Juri, A.Z.; Muhamad, S.S.; Haron, C.H.C.; Jouini, N. A Review of Sustainable Hybrid Lubrication (Cryo-MQL) Techniques in Machining Processes. *Int. J. Adv. Manuf. Technol.* **2024**, *131*, 151–169. [CrossRef]
41. Abedrabbo, F.; Soriano, D.; Madariaga, A.; Fernández, R.; Abolghasem, S.; Arrazola, P.J. Experimental Evaluation and Surface Integrity Analysis of Cryogenic Coolants Approaches in the Cylindrical Plunge Grinding. *Sci. Rep.* **2021**, *11*, 20952. [CrossRef] [PubMed]
42. Pušavec, F.; Grguraš, D.; Koch, M.; Krajnik, P. Cooling capability of liquid nitrogen and carbon dioxide in cryogenic milling. *CIRP Ann.* **2019**, *68*, 73–76. [CrossRef]
43. Shao, Y.; Fergani, O.; Ding, Z.; Li, B.; Liang, S.Y. Experimental Investigation of Residual Stress in Minimum Quantity Lubrication Grinding of AISI 1018 Steel. *J. Manuf. Sci. Eng. Trans. ASME* **2016**, *138*, 011009. [CrossRef]
44. Zhou, N.; Peng, R.L.; Pettersson, R. Surface Characterization of Austenitic Stainless Steel 304l after Different Grinding Operations. *Int. J. Mech. Mater. Eng.* **2017**, *12*, 6. [CrossRef]

45. Pušavec, F.; Hamdi, H.; Kopac, J.; Jawahir, I.S. Surface Integrity in Cryogenic Machining of Nickel Based Alloy—Inconel 718. *J. Mater. Process. Technol.* **2011**, *211*, 773–783. [CrossRef]
46. Ganesh, M.; Arunkumar, N.; Kumar, N.A.; Sathish, R. Investigation of Surface Grinding on Inconel under Distinct Cooling Conditions. *Mater. Manuf. Process.* **2023**, *38*, 1823–1836. [CrossRef]